The FASEB Journal

RESEARCH ARTICLE

Loss of the vitamin A receptor RBPR2 in mice disrupts whole-body retinoid homeostasis and the quantitative balance regulating retinylidene protein synthesis

Rakesh Radhakrishnan[1] | Matthias Leung[1] | Anjelynt Lor[1] | Swati More[2] | Glenn P. Lobo[1]

[1]Department of Ophthalmology, University of Minnesota, Minneapolis, Minnesota, USA

[2]Center for Drug Design, College of Pharmacy, University of Minnesota, Minneapolis, Minnesota, USA

Correspondence
Glenn P. Lobo, Department of Ophthalmology and Visual Neurosciences, University of Minnesota, Lions Research Building, Room LRB 225, Minneapolis, MN 55455, USA.
Email: lobo0023@umn.edu

Abstract

The distribution of stored dietary vitamin A/all-*trans*-retinol (ROL) from the liver throughout the body is critical for maintaining retinoid function in peripheral tissues and for generating visual pigments for photoreceptor cell function. ROL circulates in the blood bound to the retinol binding protein 4 (RBP4) as RBP4-ROL. Two membrane receptors, RBPR2 in the liver and other non-ocular tissues, and STRA6 in the eye are proposed to bind circulatory RBP4 and this mechanism facilitates the internalization of ROL. Herein, we conducted a longitudinal study to investigate the importance of RBPR2 and influence of vitamin A content in the diet on whole-body retinoid homeostasis and its effects on chromophore production in the support of visual function. *Rbpr2*-knockout (*Rbpr2*$^{-/-}$) and wild-type mice were fed a vitamin A sufficient (VAS) or a vitamin A deficient (VAD) diet. After 3-months of dietary intervention and compared with WT mice, *Rbpr2*$^{-/-}$ mice showed significantly lower hepatic ROL and retinyl ester content, and decreased chromophore concentrations, manifesting in dysfunctional scotopic and photopic electroretinogram (ERG) responses. These phenotypes were more severe in VAD *Rbpr2*$^{-/-}$ mice, when compared with VAS *Rbpr2*$^{-/-}$ mice. After 6 months of dietary intervention, while WT mice were able to maintain retinoid homeostasis in peripheral tissues, *Rbpr2*$^{-/-}$ mice showed elevated serum apo-RBP4 protein, decreased retinoid content in peripheral tissues including the liver and the eye causing an accumulation of apoprotein opsin in photoreceptors, which resulted in delayed rod and cone opsin regeneration. Together, our analyses characterize the molecular events underlying nutritional blindness in a novel mouse model and indicate that the vitamin A receptor, RBPR2, is required for whole-body

---

Abbreviations: 11-*cis*-RAL, 11-*cis*-retinaldehyde; *at*RA, all-*trans*-retinoic acid; HPLC, high performance liquid chromatography; LRAT, lecithin:ROL acyltransferase; RBP4, retinol-binding protein 4; RBPR2, retinol binding protein 4 receptor 2; ROL, all-*trans*-retinol; STRA6, stimulated by retinoic acid protein 6; Stra6l, stimulated by retinoic acid protein 6 like.

Rakesh Radhakrishnan and Matthias Leung contributed equally to this work.

- -

retinoid homeostasis, which supports chromophore production and visual function under variable conditions of dietary vitamin A intake throughout the lifespan of the animal.

1 | INTRODUCTION

Dietary vitamin A/all-*trans*-retinol (ROL) has pleiotropic functions in the human body, attributable to its several biologically active forms, collectively termed retinoids.[1] These functions include vision, corneal development, immune system functioning, maintaining epithelium integrity, metabolic function, cellular growth and differentiation, and fetus and central nervous system development.[1–5] Dietary vitamin A is the precursor for the visual chromophore (11-*cis*-retinaldehyde/11-*cis*-retinal) and all-*trans*-retinoic acid (a*t*RA). The vitamin A active metabolite in the eye, 11-*cis*-retinal, binds with photoreceptor opsin protein, a G-coupled protein receptor, to form rhodopsin that is the critical pigment for light perception.[4,5] Upon light exposure, 11-*cis*-retinal is isomerized to all-*trans*-retinal, causing a photobleaching process where rhodopsin forms several different intermediate states that trigger a G-protein signaling pathway. The vitamin A metabolite a*t*RA is a hormone-like molecule that regulates gene expression through interactions with nuclear receptors that are critical for the differentiation and patterning of the eyes. Vitamin A deficiency in the eye impairs night vision due to deficient rhodopsin/retinylidene protein synthesis and if left untreated can lead to photoreceptor cell death and blindness.[4,6–18] Significantly, since humans are exposed to fluctuating conditions of dietary vitamin A intake throughout their lifespan, an understanding of the mechanisms that regulate and maintain the quantitative balance of retinoids in the body are critical to help design strategies to prevent dysfunctional serum and peripheral tissue retinoid homeostasis in retinal diseases susceptibility.

The main transport form of dietary vitamin A in the circulation to peripheral tissues is all-*trans*-retinol (ROL), which is bound to the retinol-binding protein 4 (RBP4) as holo-RBP4 (RBP4-ROL).[1,2,19–20] There currently exist two membrane receptors that have been shown to bind to the RBP4-ROL complex and facilitate the internalization of ROL into tissues from the circulation. Previously, biochemical and genetic evidence have elegantly demonstrated that stimulated by retinoic acid 6 (STRA6), a

receptor that is highly expressed in the retinal pigmented epithelium (RPE), is involved in the uptake of circulatory ROL into the eye.[21–23] STRA6 is however not expressed in major peripheral/non-ocular tissues, most notably, STRA6 is not expressed in the liver despite its role as the main storage organ for dietary vitamin A.[2,24–29] These observations indicate that alternate vitamin A receptors might exist in such tissues, which may be responsible for the maintenance of liver and whole-body retinoid homeostasis. First identified by the Graham laboratory in 2013, the retinol-binding protein receptor 2, RBPR2 or STRA6like (STRA6l), is implicated in the re-uptake of ROL from circulating RBP4, in the liver and other peripheral tissues, but not in the eye due to its lack of expression there.[30] Our previous biochemical and genetic analysis of RBPR2 in cell lines, and in zebrafish and mice deficient in RBPR2 showed that it was a bona fide RBP4-ROL receptor, and is involved in ROL internalization.[26–28] Additionally, we have previously demonstrated that RBPR2 contains specific RBP4-ROL-binding motifs that suggest direct binding and association with circulatory RBP4-ROL complex.[25,28] Most critically, we have demonstrated that the loss of this systemic vitamin A transporter resulted in visual function defects in mice.[24,25] However, the long-term effects of RBPR2 has in maintaining liver and whole-body vitamin A/retinoid homeostasis are yet unknown. Therefore, given the current understanding of the mechanisms of RBPR2, we hypothesize that RBPR2 would have a direct impact in maintaining the quantitative balance between chromophore and opsins in the generation of rhodopsin for visual function, especially under conditions of dietary vitamin A insufficiency.

To answer these questions, we have now conducted a longitudinal study in $Rbpr2^{-/-}$ and WT mice fed with either a vitamin A sufficient (VAS) or vitamin A deficient (VAD) diet, to better understand the consequences of the diet and genetics on whole-body dietary vitamin A uptake and storage, and its impact on ocular retinoid homeostasis. We also aimed to investigate the long-term effects of the diet under these genotypes on chromophore production for visual function. By comparing RBPR2-deficient mice to WT mice under different conditions of dietary

vitamin A supply, we studied the physiological role of the vitamin A receptor, RBPR2, in maintaining whole-body retinoid homeostasis, which is important for visual pigment synthesis and photoreceptor cell function throughout the lifespan of humans.

2 | MATERIALS AND METHODS

2.1 | Materials

All chemicals unless stated otherwise were purchased from Sigma-Aldrich (St. Louis, MO, USA) and were of molecular or cell culture grade quality.

2.2 | Animals, animal husbandry, and diets

Rbpr2-knockout (*Rbpr2*^{-/-}) mice used in the study have been previously described.[24] Six-week-old wildtype (WT) mice (C57BL/6J) were purchased from JAX labs. Breeding pairs and litters of *Rbpr2*^{-/-} and WT mice were genotyped and found to be negative for the known *Rd8* and *Rd1* mutations, as previously described by us.[24,31] Breeding pairs of mice were fed purified breeder diets, provided water ad libitum, and maintained at 24°C in a 12:12h light–dark cycle. All animal experiments were approved by the Institutional Animal Care and Use Committee (IACUC) of the University of Minnesota (protocol # 2312-41637A) and performed in compliance with the ARVO Statement for the use of Animals in Ophthalmic and Vision Research. Post-weaning (P21), equal numbers of male and female mice were randomly distributed to different vitamin A feeding groups. For experiments, WT or *Rbpr2*^{-/-} mice were fed purified rodent diets (AIN-93G; Research Diets, New Brunswick, NJ) containing the recommended 4 IU of vitamin A/g (Vitamin A sufficient diet; VAS) or specially formulated and purified low vitamin A/vitamin A deficient (VAD) diets contained 0.22 IU vitamin A/g based on the AIN-93G diet (Research Diets, New Brunswick, NJ)[10–12,24,32] for up to 6-months.

2.3 | Immunohistochemistry and fluorescence imaging

Mice at 3- and 6-months on the variable dietary vitamin A conditions were euthanized by CO_2 asphyxiation and cervical dislocation, according to approved IACUC protocols. Eyes were enucleated and fixed with either 4% PFA in 1X PBS or in Davidson's fixative for 4h at 4°C. Paraffin-embedded retinal sections (~8 μm) were processed for antigen retrieval and immunofluorescence. Primary antibodies were diluted in 1% normal goat serum (NGS) blocking solution as follows: anti-rhodopsin 1D4 for mouse rod opsin (1:200; Abcam, St. Louis, MO, USA), R/G cone opsins (1:100; Millipore, St. Louis, MO, USA), and 4′,6-diamidino-2-phenylendole (DAPI; 1:5000, Invitrogen) or Hoechst (1:10 000, Invitrogen) to label nuclei. All secondary antibodies (Alexa Fluor 488) were used at 1:5000 concentration (Molecular Probes, Eugene, OR, USA). After mounting, images were captured using 40X and 60X objectives. Optical sections were obtained with a Nikon AXR confocal microscope and processed with the Nikon Viewer software and the acquired retinal images were calibrated with the ZEISS ZEN 3.4 software package. All fluorescently labeled retinal sections were analyzed and fluorescence within individual retinal layers were quantified using Image J or Fiji (NIH) and data were plotted in GraphPad Prism.

2.4 | Electroretinogram (ERG) analysis

2.4.1 | Dark-adapted scotopic ERG

Mice were dark-adapted overnight for 12–16h. Under single-source red light, eyes were dilated with tropicamide and phenylephrine before being sedated with Isoflurane using a calibrated Isoflurane machine (equipped with precision vaporizer, flow meter, and oxygen). A drop of 2.5% hypromellose ophthalmic demulcent solution (Systane) was placed onto the cornea just before the electroretinogram. Dark-adapted electroretinograms (ERG) were obtained (0.01–100 cd s/m^2) using a Celeris instrument (Diagnosys). Before running a combined dark and light protocol (Diagnosys Espion software), the electrodes were placed on the cornea and an impedance was measured. The Rod response recovery after bleaching, Celeris ERG protocols were performed with pulse frequency 1 and pulse intensity 1. The protocol was set to acquire prebleach amplitudes and to initiate the bleaching protocol using Light adaptation time 180 secs. After bleaching the amplitudes of the *a*- and *b*-waves were measured under scotopic conditions (1 cd s/m^2) for every minute until 10-min post-bleaching. The curves were plotted in GraphPad Prism, and the half-time was measured using the one phase association formula $Y = Y0 + (\text{Plateau} - Y0) * (1 - \exp(-K * x))$. $Y0$ is the Y value when X (time) is zero. Span is the difference between $Y0$ and Plateau, expressed in Y values. Half-time is in the time units, the amount of time needed to reach half of the maximum recovery or plateau, it is computed as $\ln(2)/K$.

2.4.2 | Light-adapted photopic ERG

Light adapted mice were sedated and eyes were dilated, as outlined in dark-adapted mice method section. To measure the photoreceptor cone response, *a*-wave, *b*-wave, and retinal ganglion response photopic ERG, Celeris ERG protocol were performed under light adapted condition with various pulse frequencies and color wavelengths. The amplitudes were recorded and plotted in GraphPad Prism.

2.5 | Purification of rhodopsin and absorbance spectroscopy

Mice were dark-adapted for 12–16 h. Under single source red light, the mice were then (CO_2) euthanized, and the retina was harvested surgically. In strict dark conditions, the retinal tissues were homogenized with 20 mM bis-tris propane, 150 mM NaCl, and 1 mM EDTA buffer pH 7.5 with protease inhibitor. The homogenates were centrifuged for 15 min at 16 000g using a refrigerated centrifuge. The supernatants were discarded, and the pellets solubilized for 1 h on a rotating platform at 4°C in 20 mM bis-tris propane, 150 mM NaCl, 20 mM n-dodecyl-b-D-maltoside (DDM) buffer and pH 7.5 with protease inhibitor. The lysate was centrifuged for 1 h at 16 000g at 4°C. The supernatant was incubated for 1 h with 30 μL HighSpec Rho1D4 MagBeads (Cat 33 299 Cube Biotech Germany). The resin was washed on a magnetic stand with 20 mM bis-tris propane, 500 mM NaCl with pH 7.5 buffer two times and three times with low salt 20 mM BTP, 100 NaCl, and 2 mM DDM buffer. The VAPA peptides dissolved in low-salt buffer were used at a concentration of 0.1 mg/mL volume 60 μL to elute the Opsins from 1D4 resin. The eluted Opsin was analyzed on an Agilent Cary 60 spectrophotometer Instrument; the measured absorbances were plotted in GraphPad Prism Version 10.1 and calculated for free Opsin using a 280/500 nm absorbance ratio,[33,34] using the extinction coefficient $\varepsilon_{500} = 40\,600\,M^{-1}\,cm^{-1}$. The concentration of ligand-free opsin was calculated using the extinction coefficient $\varepsilon_{280} = 81\,200\,M^{-1}\,cm^{-1}$.

2.6 | High-performance liquid chromatography (HPLC) analyses of retinoids

Retinoid isolation procedures were performed under a dim red safety light (600 nm) in a dark room. Animals were first euthanized with CO_2 asphyxiation, and pertinent tissues were removed from the carcass. The tissue (eyes or peripheral tissues) was then homogenized in 0.9% saline with a handheld tissue grinder, consisting of a glass tube and glass pestle. Methanol (2 mL) was added into the homogenate to precipitate the proteins within the homogenate. For separation and detection of retinaldehydes in ocular tissue, 1 mL of 0.1 M hydroxylamine hydrochloride in 0.1 M HEPES (pH 6.5) was additionally added to the homogenate and left for 15 minutes at room temperature to convert retinaldehyde into retinal oximes. This step is otherwise not necessary in all other tissues since retinals are not readily present in them.[35,36] The retinoid content from the tissue (peripheral organs) homogenate was then extracted with 10 mL of hexane (twice), with the aqueous layer subsequently removed. The combined hexane extracts were then evaporated with a vacuum evaporator, re-suspended in 100 μL of hexane, then injected into an HPLC for analysis. HPLC analysis was performed on an Agilent 1260 Infinity HPLC with a UV detector. The HPLC conditions employed two normal-phase Zorbax Sil (5 μm, 4.6 × 150 mm) columns (Agilent, Santa Clara, CA, USA), connected in series within the Multicolumn Thermostat compartment. Chromatographic separation was achieved by isocratic flow of mobile phase containing 1.4% 1-Octanol/2% 1,4-Dioxane/11.2% Ethyl Acetate/85.4% Hexane, at a flow rate of 1 mL/min for 40 min. Retinaldehydes, retinol, and retinyl esters were detected at 325 nm using a UV–Vis DAD detector, while the UV absorbance spectra was collected from 200 to 700 nm.[35,36] For quantifying molar amounts of retinoids, the HPLC was previously calibrated with synthesized standard compounds and as previously described by us. Calculation of concentration (μM): Standards were injected in concentrations ranging from 0 to 3.5 μM prepared solutions in the mobile phase. The plotted concentrations were fit through linear regression to obtain R-equation ($y = mx + c$) where y is the peak area (mAU s); m is the slope of the calibration curve and c is the y-intercept. The area from the HPLC peaks of the samples (mAU s) are interpolated into concentration and expressed as picomoles. For eyes, the values are expressed as picomoles/eye; for liver, lung, spleen, and kidney the values are expressed as picomoles/mg of tissue; for serum, the ROL values are expressed as picomoles/microliter.

$$\text{Concentration X (picomoles)} = \frac{\text{Peak area } y \text{ (mAU s)} + y\text{-intercept}}{\text{Slope (m)}}$$

2.7 | Statistical analysis

Data were expressed as means ± standard error mean, statistical analysis by ANOVA and student *t*-test. Differences between means were assessed by Tukey's honestly significant difference (HSD) test. *p*-values below 0.05 ($p < .05$) were considered statistically

significant. For western blot analysis, the relative intensities of each band were quantified (densitometry) using the Image *J* software version 1.54 and normalized to Ponceau S stain. Statistical analysis was carried out using GraphPad Prism v 10.1.

3 | RESULTS

### 3.1 | Design of mouse studies and dietary vitamin A intervention

In this study, we used our previously established RBPR2-deficient ($Rbpr2^{-/-}$) mouse line and isogenic C57BL/6J wild-type (WT) mice.[24] Breeding pairs and litters of $Rbpr2^{-/-}$ and WT mice were genotyped and found to be negative for the known *Rd8* and *Rd1* mutations.[24] Each group had equal number of male and female mice and were randomly assigned to different dietary vitamin A groups. Groups of WT and $Rbpr2^{-/-}$ mice were fed either a vitamin A sufficient (VAS; 4 IU vitamin A/g) or vitamin A deficient (VAD; 0.22 IU/g) diet post-weaning at P21, which are custom diets routinely used to control vitamin A status in mice.[32,37] Additionally, the 4 IU vitamin A/g concentration in the VAS diet is consistent with the recommended vitamin A intake for rodents and corresponds to 1.2 mg retinol activity equivalent (RAE), which is also a recommended intake in humans. After 3-months of dietary intervention, the first cohort of mice were sacrificed to determine the short-term effects, while the second cohort of mice were sacrificed after 6-months of dietary intervention to determine the long-term effects of dietary vitamin A deficiency on whole-body all-*trans*-retinol uptake and liver storage as retinyl esters (RE) and on ocular retinoids and health in the different genotypes (Figure 1).

3.2 | Total retinoid concentrations are decreased in the liver of $Rbpr2^{-/-}$ mice

We and others have shown in mice that unlike STRA6, the vitamin A receptor, RBPR2, is highly expressed in the liver and to a lesser extent in non-ocular peripheral tissues.[2,20,24,25,30,38,39,40] Therefore, we first examined how global loss of RBPR2 in mice affects ROL and RE levels in the liver by high-performance liquid chromatography (HPLC) analysis and compared these results to age-matched wild-type (WT) mice. At the early timepoint (3-month), we observed that ROL, retinyl esters (RE), and total retinoid concentrations in the liver of VAS $Rbpr2^{-/-}$ mice were similar to those of age-matched WT mice (Figure 2A–E). However, while VAD WT mice were able to maintain liver retinoid homeostasis, VAD $Rbpr2^{-/-}$ mice showed significant reductions in total retinoid concentration (Figure 2E).

We then investigated the long-term effects of RBPR2 loss on liver retinoid homeostasis, at the 6-month timepoint. In WT mice under either vitamin A diets, ROL, RE, and total retinoid concentrations in the liver were not affected (Figure 3A–D). However, RE concentration in the liver
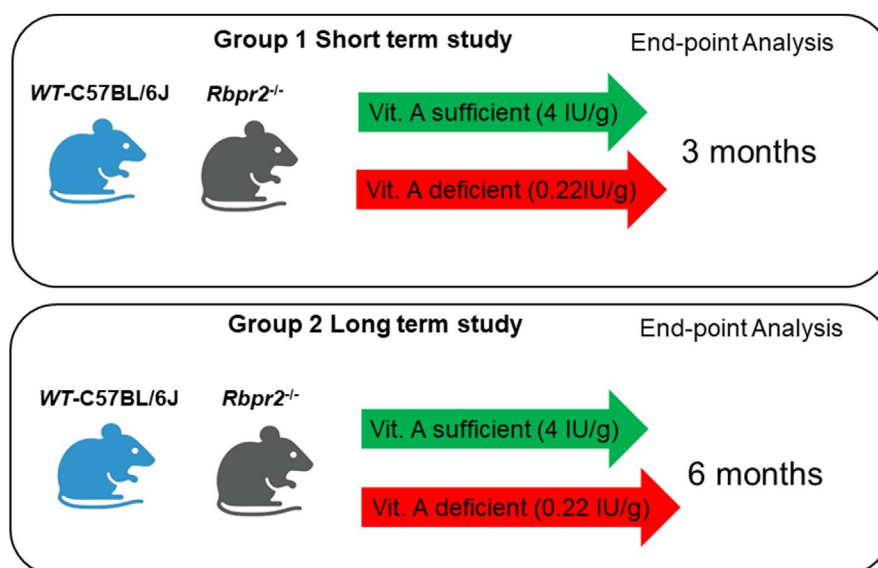
FIGURE 1 Schematic overview of the mouse study and vitamin A diet intervention. Post-weaning, we fed cohorts of WT and $Rbpr2^{-/-}$ mice with a vitamin A sufficient (VAS) or vitamin A deficient (VAD) diet. At the 3-month (early timepoint analysis) and 6-month timepoint (late timepoint analysis) of dietary vitamin A intervention, noninvasive tests for retinal function and integrity were performed. High performance liquid chromatography (HPLC) analysis for the quantification of retinoids was then performed on ocular and multiple non-ocular tissues.
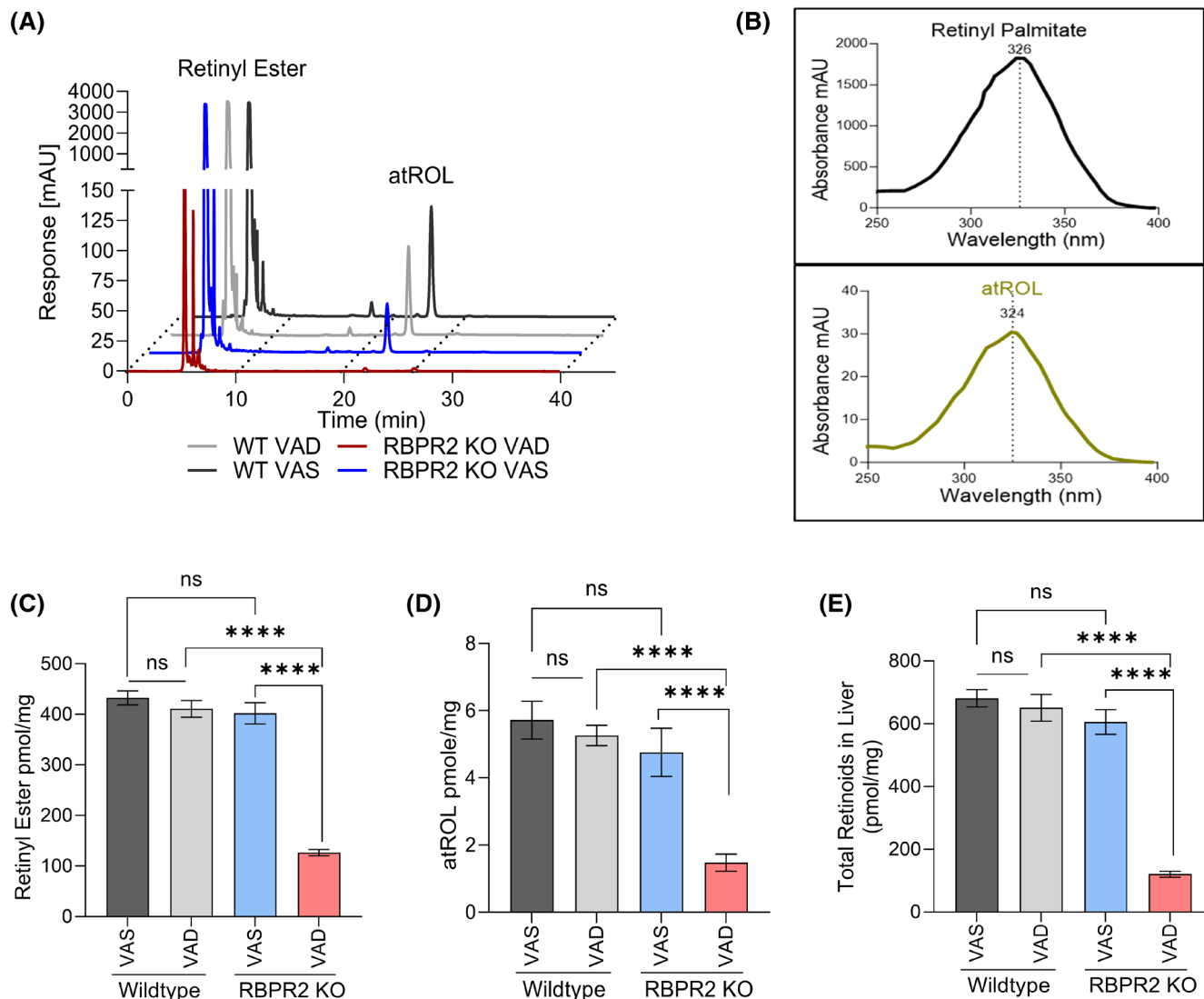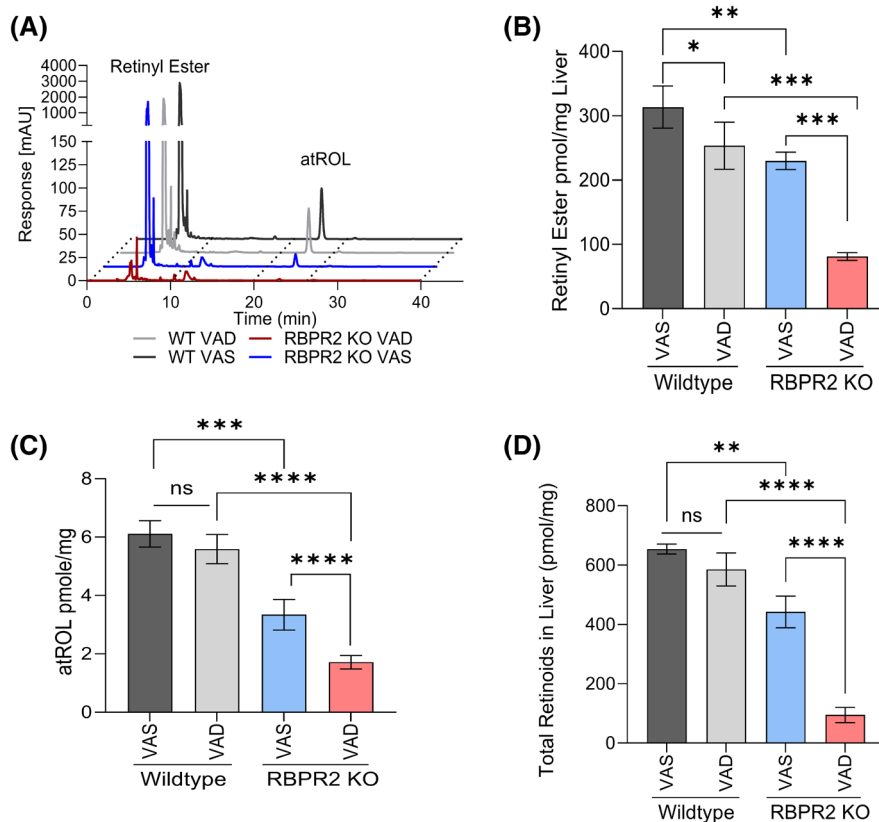
FIGURE 2 Quantification of total retinoids in livers of mice post 3-months dietary vitamin A feeding regime. High performance liquid chromatography (HPLC) analysis and quantification of all-*trans*-ROL (ROL), retinyl esters (RE), and total retinoid content in livers isolated from VAS and VAD WT and *Rbpr2*$^{-/-}$ mice post 3-months of feeding. (A) HPLC chromatograms and (B) absorbance spectra of individual retinoids, (C) Retinyl esters, (D) all-*trans*-retinol, and (E) total retinoids in the liver. Values are presented as ±SD. Two-way ANOVA, ****$p < .001$; ns, not significant. VAD, vitamin A-deficient diet; VAS, vitamin A sufficient diet; WT, wild-type mice. $n = 6$–8 animals per group and dietary condition.

was lower in VAD WT mice, compared with VAS WT mice, indicating that stored RE was converted back to ROL and re-distributed under the prolonged vitamin A restriction condition (Figure 3B). Conversely, in VAS and VAD *Rbpr2*$^{-/-}$ mice, ROL, RE, and total retinoid concentrations in the liver were lower when compared with WT mice (Figure 3A–D). Likewise, total retinoids in the liver of VAD *Rbpr2*$^{-/-}$ mice compared with VAS *Rbpr2*$^{-/-}$ mice were severely depleted at the 6-month timepoint. These results indicate that RBPR2 likely plays a significant role in maintaining retinoid homeostasis under variable conditions of dietary vitamin A intake, and also that *Rbpr2*$^{-/-}$ mice are more susceptible to dietary vitamin A deficiency, which in the long-term, affects liver retinoid stores (Figures 2 and 3).

3.3 | Serum RBP4-ROL complex homeostasis is impaired in *Rbpr2*$^{-/-}$ mice

Since liver ROL/RE concentrations were significantly decreased in *Rbpr2*$^{-/-}$ mice at the 6-month timepoint (Figure 3B–3D), we next determined if this could affect serum RBP4-ROL complex homeostasis. To test this, we obtained serum from age-matched *Rbpr2*$^{-/-}$ and WT mice at the 6-month timepoint (from above) and performed western blot analysis using a commercial RBP4 antibody. This analysis showed that while WT mice were able to maintain RBP4 protein homeostasis under variable conditions of dietary vitamin A intake, conversely *Rbpr2*$^{-/-}$ mice showed higher RBP4 protein

FIGURE 3 Quantification of total retinoids in livers of mice post-6-months dietary vitamin A feeding regime. High performance liquid chromatography (HPLC) analysis and quantification of all-*trans*-ROL (ROL), retinyl esters (RE), and total retinoid content in livers isolated from VAS and VAD WT and *Rbpr2*$^{-/-}$ mice post-6-months of feeding. (A) HPLC chromatograms of individual retinoids in liver. (B) Quantification of hepatic retinyl ester. (C) Quantification of hepatic all-*trans*-retinol. (D) Quantification of total retinoids in the liver. Values are presented as ±SD. Two-way ANOVA, *$p < .05$; **$p < .01$; ***$p < .005$; ****$p < .001$; ns, not significant. VAD, vitamin A-deficient diet; VAS, vitamin A sufficient diet; WT, wild-type mice. $n = 6–8$ animals per group and dietary condition.

3.4 | Total retinoid concentrations are decreased in peripheral tissues of *Rbpr2*$^{-/-}$ mice

Since *Rbpr2*$^{-/-}$ mice showed dysregulated serum RBP4-ROL complex homeostasis, we sought to investigate the long-term effects of this disruption on retinoid homeostasis in peripheral tissues, previously shown to express RBPR2.[24,30] To investigate these hypotheses, we isolated lung, spleen, and kidney, the peripheral tissues known in the serum (Figure 4A,B). HPLC analysis showed that while serum all-*trans*-retinol concentrations were homeostatically maintained in VAS and VAD WT animals, they were significantly reduced in VAS and VAD *Rbpr2*$^{-/-}$ mice (Figure 4C). Quantification of the molar ratio of serum RBP4 to ROL showed no differences in VAS or VAD WT mice, in contrast to *Rbpr2*$^{-/-}$ mice, where lower serum ROL concentrations and higher RBP4 protein indicated the presence of unliganded/apo-RBP4 protein (Figure 4D,E). Thus, while WT mice can maintain serum RBP4-ROL complex homeostasis under variable conditions of dietary vitamin A intake, the absence of RBPR2 made mice susceptible to serum ROL deficiency, which could influence peripheral tissue retinoid homeostasis.

store vitamin A and contain notable amounts of RE. These tissues were extracted from WT and *Rbpr2*$^{-/-}$ mice at the 6-month timepoint and HPLC analysis was performed to quantify total retinoids. This analysis showed that while WT mice were able to maintain retinoid homeostasis in peripheral tissues under variable conditions of dietary vitamin A intake, *Rbpr2*$^{-/-}$ mice showed lower total retinoids in these tissues, which were more severely depleted in VAD *Rbpr2*$^{-/-}$ mice (Figure 5A–C). Thus, our data suggest that RBPR2 is required to maintain retinoid homeostasis in serum and peripheral tissues, especially under conditions of dietary vitamin A restriction.

3.5 | Consequences of RBPR2 loss on ocular retinoid pool and visual function

We next investigated the short-term and long-term consequences of dysregulated liver, serum, and peripheral tissue retinoid homeostasis in *Rbpr2*$^{-/-}$ mice on ocular retinoid concentrations and on visual function and compared these observations to WT mice. In the eyes of VAS and VAD WT mice at the 3-month timepoint, total retinoid concentrations were unchanged. Similarly, VAS *Rbpr2*$^{-/-}$ mice were able to maintain ocular retinoid homeostasis, in contrast to VAD *Rbpr2*$^{-/-}$ mice,
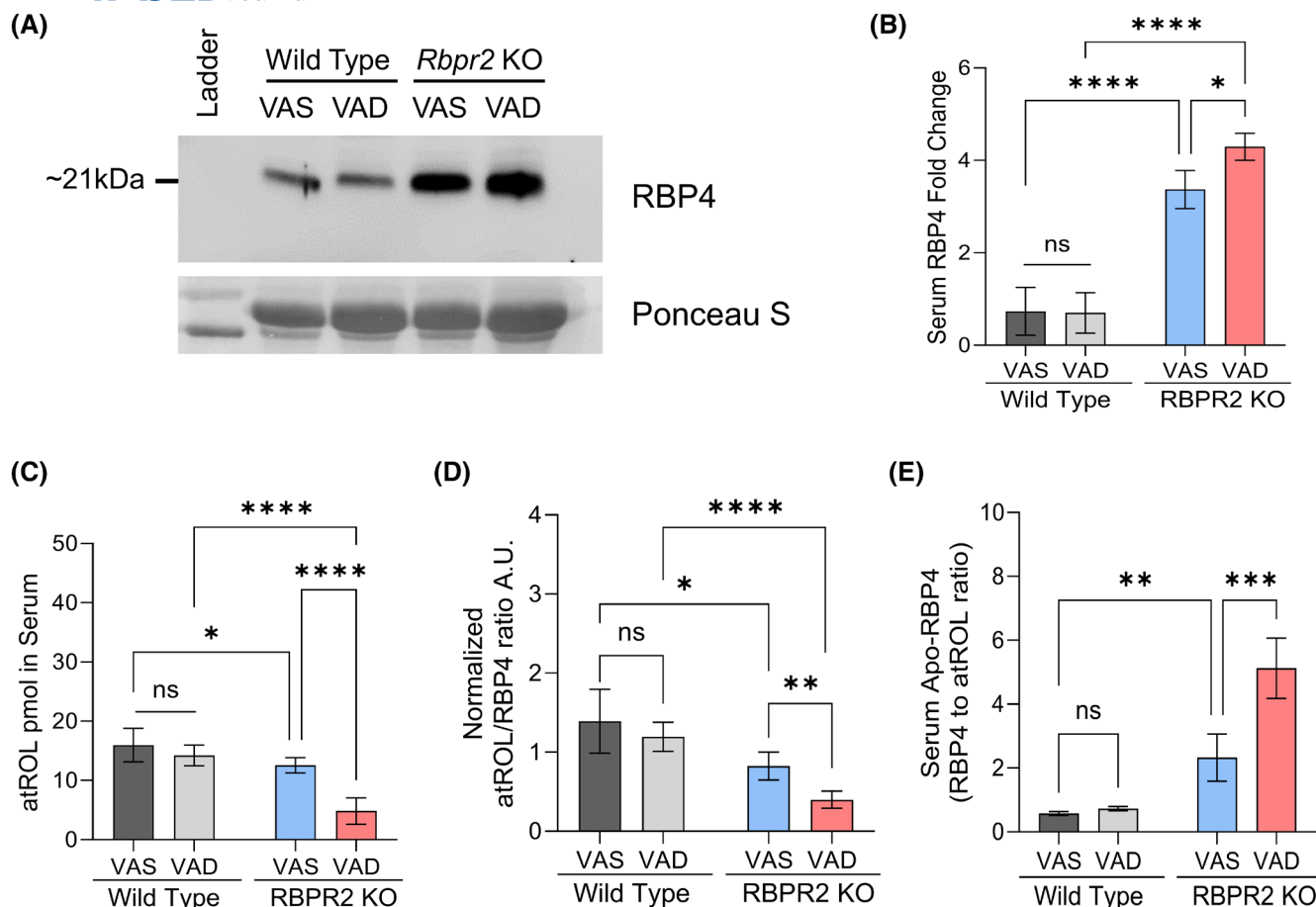
FIGURE 4 Analysis of serum RBP4-ROL complex in mice at 6-months post-dietary vitamin A feeding regime. (A and B) Western blot analysis and quantification of serum RBP4 protein in VAS and VAD WT and *Rbpr2$^{-/-}$* mice post 6-months of feeding. (C) Quantification of all-*trans*-retinol concentration in serum. (D) Normalized RBP4:ROL molar ratios. (E) Estimation of circulatory ROL free RBP (apo-RBP4) protein in serum. Two-way ANOVA, *$p < .05$; **$p < .01$; ***$p < .005$; ****$p < .001$; ns, not significant. VAD, vitamin A-deficient diet; VAS, vitamin A sufficient diet; WT, wild-type mice. $n = 6–8$ animals per group and dietary condition.

which showed significantly depleted ocular retinoids (Figure 6A–C). We next recorded the electrical responses to light generated by rod photoreceptors, in dark-adapted mice eyes of *Rbpr2$^{-/-}$* and WT mice, fed either a VAS or VAD diet, and the responses generated by cones in light-adapted eyes, by electroretinography (ERG) ranging from 0.01–100 cd.s/m². ERG analysis showed that scotopic *a*-wave and *b*-wave amplitudes were significantly decreased in 3-month-old VAD *Rbpr2$^{-/-}$* mice, compared with VAS *Rbpr2$^{-/-}$* or WT mice (Figure 6D–G). In the eyes of WT mice at the 6-month timepoint, total ocular retinoid concentrations were unchanged. Conversely, in VAS and VAD *Rbpr2$^{-/-}$* mice, total retinoid concentrations were significantly lower compared with WT mice (Figure 7A). WT mice showed no changes in ERG amplitudes under either diet, however, *Rbpr2$^{-/-}$* mice showed an even more severe decrease in *a*-wave and *b*-wave visual responses at the 6-month timepoint, compared with WT mice (Figure 7B–E).

3.6 | Rod photoreceptors of *Rbpr2$^{-/-}$* mice display significant levels of apoprotein opsin

Since Rbpr2$^{-/-}$ mice display reduced visual responses, we hypothesized that this phenotype is caused by imbalances between chromophore and opsin concentrations in rod photoreceptors, which may also result in the accumulation of unliganded/apoprotein opsin in photoreceptor inner segments (IS). We first analyzed the localization of rhodopsin in retinal sections, from WT mice compared with *Rbpr2$^{-/-}$* mice, by immunohistochemistry (IHC) at 6 months of age. In VAS and VAD WT mice, rhodopsin was properly localized to the photoreceptor outer segments (Figure 8A). Conversely, in VAS and VAD *Rbpr2$^{-/-}$* mice, the presence of mislocalized rod opsins was evident in the photoreceptor IS, which was more severe in VAD *Rbpr2$^{-/-}$* mice (Figure 8A,F).

We next determined the levels of unliganded/apoprotein opsin by performing UV–visible spectrophotometry with the isolated retinal protein fractions from WT and
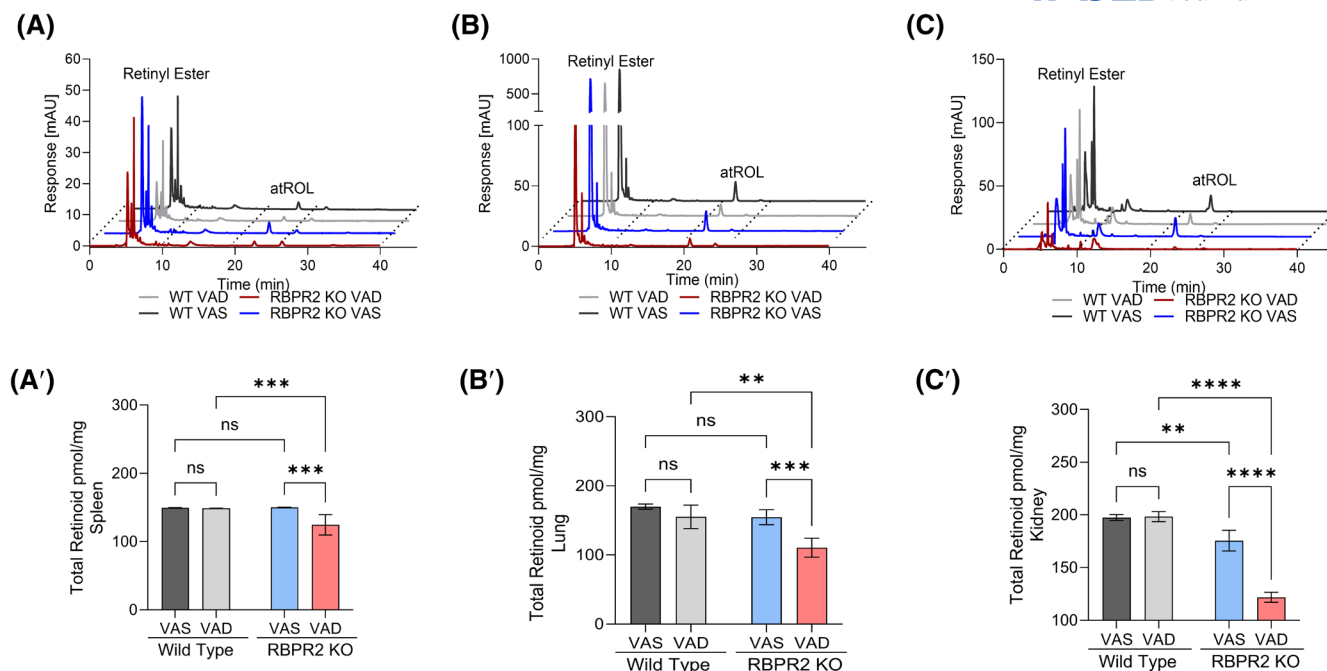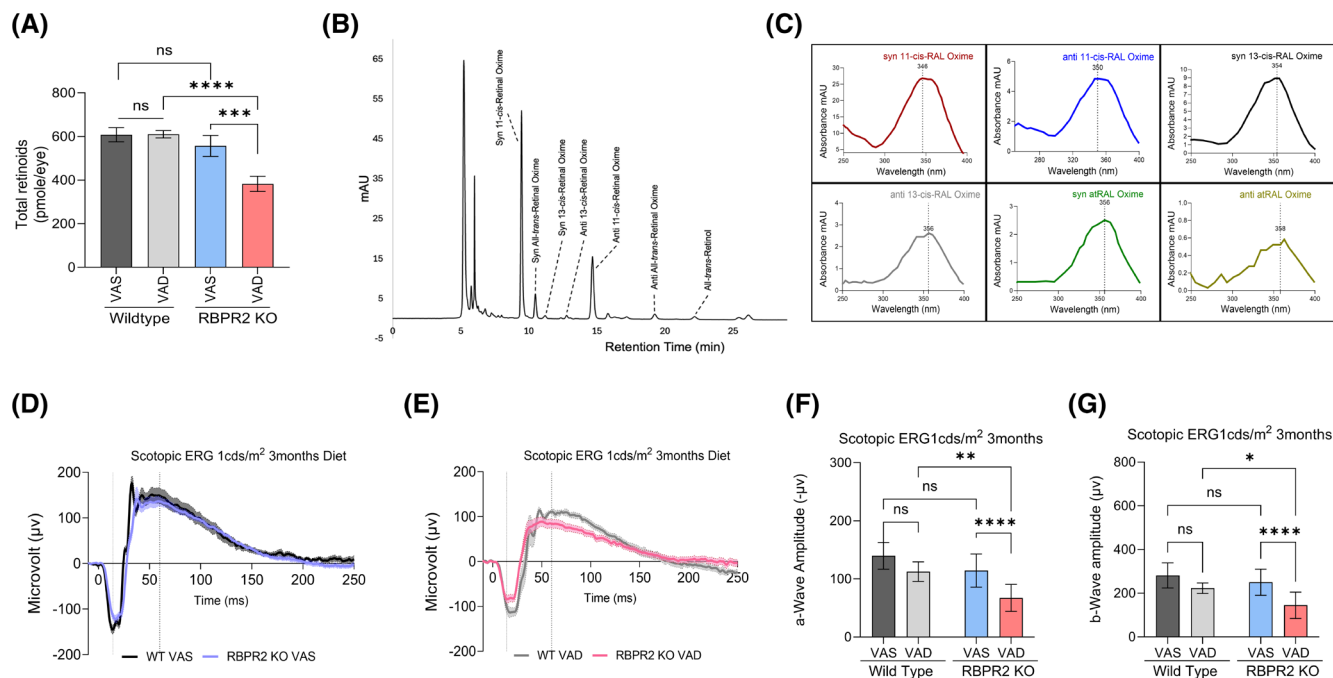
FIGURE 5 Quantification of total retinoids in peripheral tissues of mice post 6-months dietary vitamin A feeding regime. High performance liquid chromatography (HPLC) analysis and quantification of total retinoid content in peripheral tissues isolated from VAS and VAD WT and *Rbpr2*$^{-/-}$ mice post 6-months of feeding. (A and A') Spleen, (B and B') Lung, and (C and C') Kidney. Values are presented as ±SD. Two-way ANOVA, **$p < .01$; ***$p < .005$; ****$p < .001$; ns, not significant. VAD, vitamin A deficient diet; VAS, vitamin A sufficient diet; WT, wild-type mice. $n = 6–8$ animals per group and dietary condition.

Rbpr2$^{-/-}$ mice using 1D4 antibody and compared the theoretical 280/500 nm ratio with the experimental ratio of absorbance.[33,34,41] We observed an ~31% and ~18% decrease in rhodopsin concentrations in dark-adapted photoreceptors of *Rbpr2*$^{-/-}$ mice fed either a VAD or VAS diet and compared with age-matched WT mice on VAS or VAD diets, respectively (Figure 8B,D). Similar results were observed in light-adapted photoreceptors, where lower Meta II rhodopsin concentrations were observed in *Rbpr2*$^{-/-}$ mice compared with WT mice on either diet (Figure 8C,E). Quantification of unliganded opsin in dark-adapted retinas showed that *Rbpr2*$^{-/-}$ mice had significant amounts of apoprotein opsin; compared to WT mice on either diet (Figure 8G). It has been proposed previously that accumulation of apoprotein opsin/unliganded opsin can activate the phototransduction cascade even under dark conditions.[13–15,18,33] The constitutive activity of apoprotein opsin in photoreceptors is considered equivalent to background light and can result in a reduction in phototransduction gain.[17,18,42] Thus, long-term loss of RBPR2 might contribute to delayed rod and cone opsin kinetics, which were tested below.

3.7 | Delayed rhodopsin regeneration in eyes of *Rbpr2*$^{-/-}$ mice

Since WT mice can maintain whole-body and ocular retinoid homeostasis under variable conditions of dietary vitamin A intake, we next focused on defining the consequences of decreased ocular retinoid pool on rhodopsin and cone opsin regeneration in 6-month *Rbpr2*$^{-/-}$ mice. Kinetic measurement of rod opsin recovery was found to be slower in VAD *Rbpr2*$^{-/-}$ mice compared with VAS *Rbpr2*$^{-/-}$ mice, likely resulting from the decreased ocular retinoid (11-*cis*-retinal) pool, which in turn resulted in delayed rhodopsin recovery after light exposure (Figure S1). We next determined ERG responses in light-adapted *Rbpr2*$^{-/-}$ mice fed either the VAS or VAD diets under different light source color (green, red, white, and UV/blue). Under photopic light conditions, ERG responses of *Rbpr2*$^{-/-}$ mice under green, white, and UV color sources were significantly diminished at the 3-month timepoint, while red light source ERG responses were not changed, when compared with WT mice on VAS diets (Figure S2A–D). Light-adapted ERG responses for green and white light
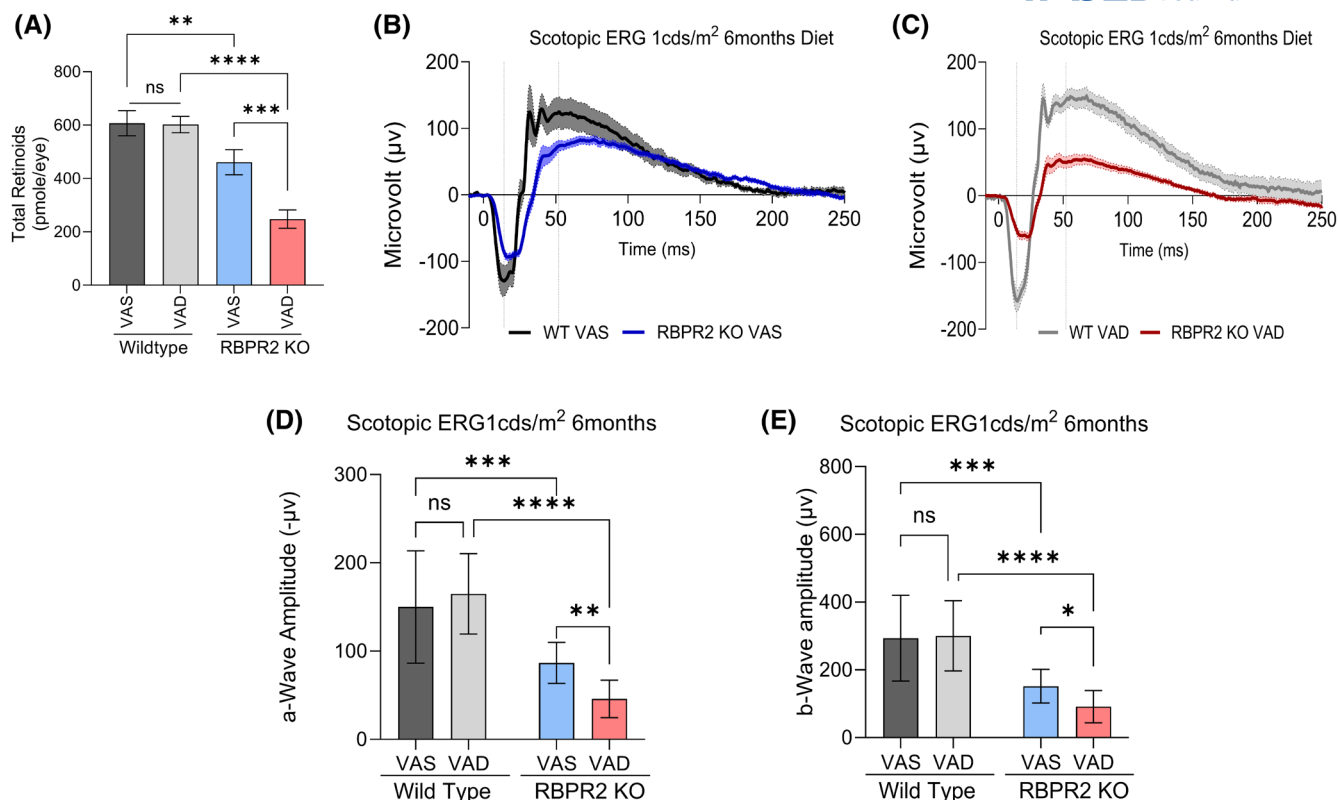
FIGURE 6 Quantification of total retinoids in eyes and tests for visual function of WT and *Rbpr2*$^{-/-}$ mice post 3-months dietary vitamin A feeding regime. High performance liquid chromatography (HPLC) analysis and quantification of total retinoid content in eyes isolated from VAS and VAD WT and *Rbpr2*$^{-/-}$ mice post-3-months of feeding. (A) Total retinoids, (B) HPLC chromatograms, and (C) absorbance spectra of individual retinoids in mice eyes. (D) Scotopic ERG responses of WT and *Rbpr2*$^{-/-}$ mice fed either a VAS diet or (E) VAD diet, showing the dark-adapted ERG responses of rod photoreceptor cell function by *a*-wave amplitudes (F), and inner neuronal bipolar cell function by *b*-wave amplitude (G). Values are presented as ±SD. Two-way ANOVA, $*p < .05$; $**p < .01$; $***p < .005$; $****p < .001$; ns, not significant. VAD, vitamin A-deficient diet; VAS, vitamin A sufficient diet; WT, wild-type mice. $n = 8$–10 animals per group and dietary condition.

intensity improved in *Rbpr2*$^{-/-}$ mice under VAS diets at the 6-month timepoint but remained significantly diminished under blue/ UV-light exposure (Figure S2A'–D'). IHC for red–green opsins (Opn1mw) in photoreceptors showed that in VAS and VAD WT mice, cone opsins were properly localized to the photoreceptor outer segments (Figure S2E). Conversely, in *Rbpr2*$^{-/-}$ mice fed either a VAS or VAD diet, the presence of mislocalized cone opsins were evident in the photoreceptor inner segments, where VAD *Rbpr2*$^{-/-}$ mice showed not only more severe cone opsin mislocalization but also shorter cone OS length (Figure S2E,F). Kinetic measurement of cone opsin recovery under photopic blue light were slower in VAD *Rbpr2*$^{-/-}$ mice, when compared with VAS *Rbpr2*$^{-/-}$ mice (Figure S3). Thus, the VAD status in *Rbpr2*$^{-/-}$ mice made them more susceptible to delayed rod and cone opsin regeneration and OS phenotypes.

4 | DISCUSSION

In this study, we investigated the whole-body and ocular consequences resulting from loss of the vitamin A receptor, RBPR2, on a longitudinal timescale. Previously, we have established a global *Rbpr2*-knockout (*Rbpr2*$^{-/-}$) mouse and have demonstrated that these mice are susceptible to visual deficiencies.[19] Here, we sought to expand upon that study in several critical ways. First, through a normal phase HPLC, we can resolve retinol, retinyl esters, and retinaldehyde individually, rather than simply quantify total retinoid content. This is especially important for retinoid analysis in peripheral and ocular tissues and allows us to directly detect and quantify critical retinoids such as retinyl esters (the major storage form of dietary ROL) and 11-*cis*-retinaldehyde, the visual chromophore responsible for generation of the retinylidene protein that is critical for phototransduction.[36] Second, we have performed this analysis on multiple systemic tissues across multiple organs systems, rather than only in ocular tissue. Given that RBPR2 is hypothesized to regulate systemic vitamin A homeostasis, we aimed to examine the changes to whole-body retinoid content in *Rbpr2*$^{-/-}$ mice. Third, to investigate the underlying causes for reduced ERG responses in *Rbpr2*$^{-/-}$ mice, we utilized UV–Vis spectrophotometry to determine whether the ocular levels of vitamin A affect the stoichiometric balance between GPCR protein opsin and the visual chromophore, 11-*cis*-retinal, in the photoreceptors.

FIGURE 7 Quantification of total retinoids in eyes and tests for visual function of WT and $Rbpr2^{-/-}$ mice post-6-months dietary vitamin A feeding regime. High performance liquid chromatography (HPLC) analysis and quantification of all-*trans*- ROL (ROL), retinyl esters (RE), retinaldehyde, and total retinoid content in eyes isolated from VAS and VAD WT and $Rbpr2^{-/-}$ mice post-6-months of feeding. (A) Total retinoids in mice eyes. Scotopic ERG responses of WT and $Rbpr2^{-/-}$ mice fed either a VAS diet (B) or VAD diet (C), showing the dark-adapted ERG responses of rod photoreceptor cell function by *a*-wave amplitudes (D) and inner neuronal bipolar cell function by *b*-wave amplitude (E). Values are presented as ±SD. 2-way ANOVA, $*p < .05$; $**p < .01$; $***p < .005$; $****p < .001$; ns, not significant. VAD, vitamin A-deficient diet; VAS, vitamin A sufficient diet; WT, wild-type mice. $n = 8–10$ animals per group and dietary condition.

To investigate if loss of RBPR2 affected serum and whole-body retinoid concentration, we performed HPLC analysis for retinoids in various peripheral tissues, including the liver, eye, spleen, kidney, and lungs, obtained from wild-type (WT) and $Rbpr2^{-/-}$ mice, fed varying concentrations of dietary vitamin A. In all analyzed tissues, all-*trans*-retinol (ROL) and its storage form, retinyl esters (RE), were the predominant retinoid found in all analyzed systemic tissue, apart from retinaldehydes in ocular tissue. Hence, quantification of ROL and RE will serve as a viable metric for determination of retinoid levels in these tissues. HPLC analysis showed that wild-type (WT) mice at both 3- and 6-month timepoints can regulate ROL and RE (total retinoids) levels in the liver, even when subjected to variable vitamin A diets (Figures 2 and 3). However, while VAS $Rbpr2^{-/-}$ mice at the 3-month timepoint can maintain similar levels of total retinoids in the liver compared with WT mice, the retinoid quantity in liver of VAS and VAD $Rbpr2^{-/-}$ mice at the 6-month significantly decreases (Figure 3D). Retinoid metabolism, like many other biochemical pathways, contains redundant pathways

(Figure 9). In particular, circulatory RE within chylomicrons originating from the VAS diet provides the most likely explanation for the maintenance of RE levels comparable to WT in VAS $Rbpr2^{-/-}$ mice at the 3-month timepoint, since this pathway can bypass the loss of RBPR2. Similar observations were obtained in $Stra6^{-/-}$ mice fed a high vitamin A diet.[29,33] However, for the $Rbpr2^{-/-}$ mice fed a VAD diet, this supplementary pathway does not exist. Once residual retinoid/RE stores from gestation run out at the 6-month timepoint, VAS, and VAD $Rbpr2^{-/-}$ mice exhibit decreased ROL and RE levels, which become severely depleted under the VAD diets.

We next examined if serum retinoid homeostasis was affected in $Rbpr2^{-/-}$ mice. While VAS and VAD WT mice were able to maintain serum ROL and RBP4 protein homeostasis even under variable conditions of dietary vitamin A intake, both VAS and VAD $Rbpr2^{-/-}$ mice at the 6-month timepoint, showed higher RBP4 protein and decreased ROL concentrations (Figure 4A–C). Further analysis showed that WT mice displayed relatively equal RBP4 to ROL molar ratios, while $Rbpr2^{-/-}$ mice showed
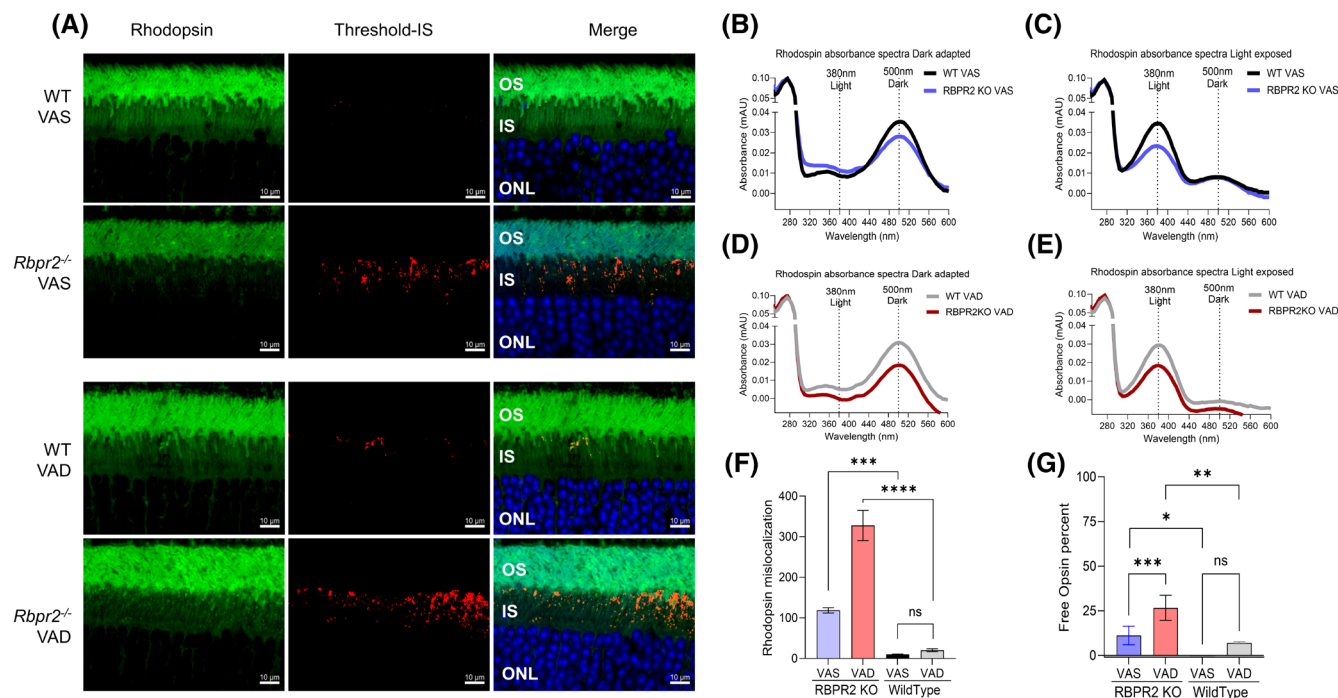
FIGURE 8 Presence of apoprotein opsin in rod photoreceptors of *Rbpr2*$^{-/-}$ mice. (A) IHC staining for rhodopsin (green) in photoreceptors and mislocalization in IS analyzed by the threshold in red, outer nuclear layer (ONL) stained with DAPI in blue and merged images showing the localization of mislocalized rhodopsin. (B) Rhodopsin absorbance spectra in dark-adapted (500 nm) animals fed either a VAS diet or (D) the VAD diet. (C) Rhodopsin absorbance spectra in light-exposed (380 nm) animals fed either a VAS diet or (E) the VAD diet. (F) Threshold-based quantification of mislocalized rhodopsin in the IS of retinas from WT and *Rbpr2*$^{-/-}$ mice fed different vitamin A diets. (G) Free opsin quantification shows the 11-*cis*-retinal free apoprotein opsin percentage in the retinas of *Rbpr2*$^{-/-}$ mice compared to WT mice. VAD, vitamin A deficient diets; VAS, vitamin A sufficient diets. Values are presented as ±SD. Two-way ANOVA, $*p < .05$; $**p < .01$; $***p < .005$; $****p < .001$. $n = 8$–10 animals per group and dietary condition.

dysfunctional RBP4 to ROL molar ratios, which indicate the presence of apo-protein RBP4 (Figure 4D,E). Thus, while WT mice were able to maintain serum RBP4: ROL complex homeostasis, loss of RBPR2 affected serum ROL and RBP4 protein complex homeostasis. To determine if dysfunctional serum RBP4:ROL complex in *Rbpr2*$^{-/-}$ mice affected peripheral retinoid homeostasis, we performed HPLC for total retinoids in key vitamin A storage organs (lung, kidney, and spleen), which are known to express RBPR2. This analysis showed that while VAS and VAD WT mice were able to maintain retinoid homeostasis, in contrast, age-matched *Rbpr2*$^{-/-}$ mice at the 6-month timepoint showed decreased total retinoids in these organs. Thus, loss of RBPR2 affected not only the liver and serum retinoid homeostasis but also negatively affected peripheral tissue retinoid concentrations.

We next examined the retinoid supply and consumption axis in the support of visual function by examining retinoid pool in the eye of *Rbpr2*$^{-/-}$ mice. This overall pattern of depressed levels of retinoids for *Rbpr2*$^{-/-}$ mice in both serum and hepatic tissue is thus reflected in ocular tissue where the total retinoid content (ROL, RE, and 11-*cis*-retinal) was found to be significantly lower in VAD

Rbpr2$^{-/-}$ mice at the 3-month timepoint, which became severely depleted in both VAS and VAD *Rbpr2*$^{-/-}$ mice at the 6-month timepoint (Figure 6A vs. Figure 7A). More critically, these depressed serum, liver, and ocular retinoid levels coexist with changes on the phenotypic level, with *Rbpr2*$^{-/-}$ mice at the 6-month timepoint exhibiting decreased rod ERG responses (Figure 7), mislocalized opsins within photoreceptor inner segments (Figure 8A), and increased ratios of unliganded/apoprotein opsin (Figure 8B–F). Previous investigations into mice exhibiting disruptions in the generation of 11-*cis*-retinal have displayed phenotypes such as elevated levels of apoprotein opsins and subsequent retinal degeneration, such as in mice with disrupted *Stra6* and *Rpe65*.[14,15,17,33] In particular, *Rpe65*$^{-/-}$ mice, a mouse model for the retinal degenerative disease Leber Congenital Amaurosis, has been shown to exhibit an elevated concentration of apoprotein opsin. RPE65 is an isomerohydrolase responsible for the conversion of retinyl esters to 11-*cis*-retinol within the visual cycle, which is in turn necessary for the generation of 11-*cis*-retinal chromophore in photoreceptors. The authors of that study have attributed the cause of retinal degeneration in *Rpe65*$^{-/-}$ mice to elevated levels
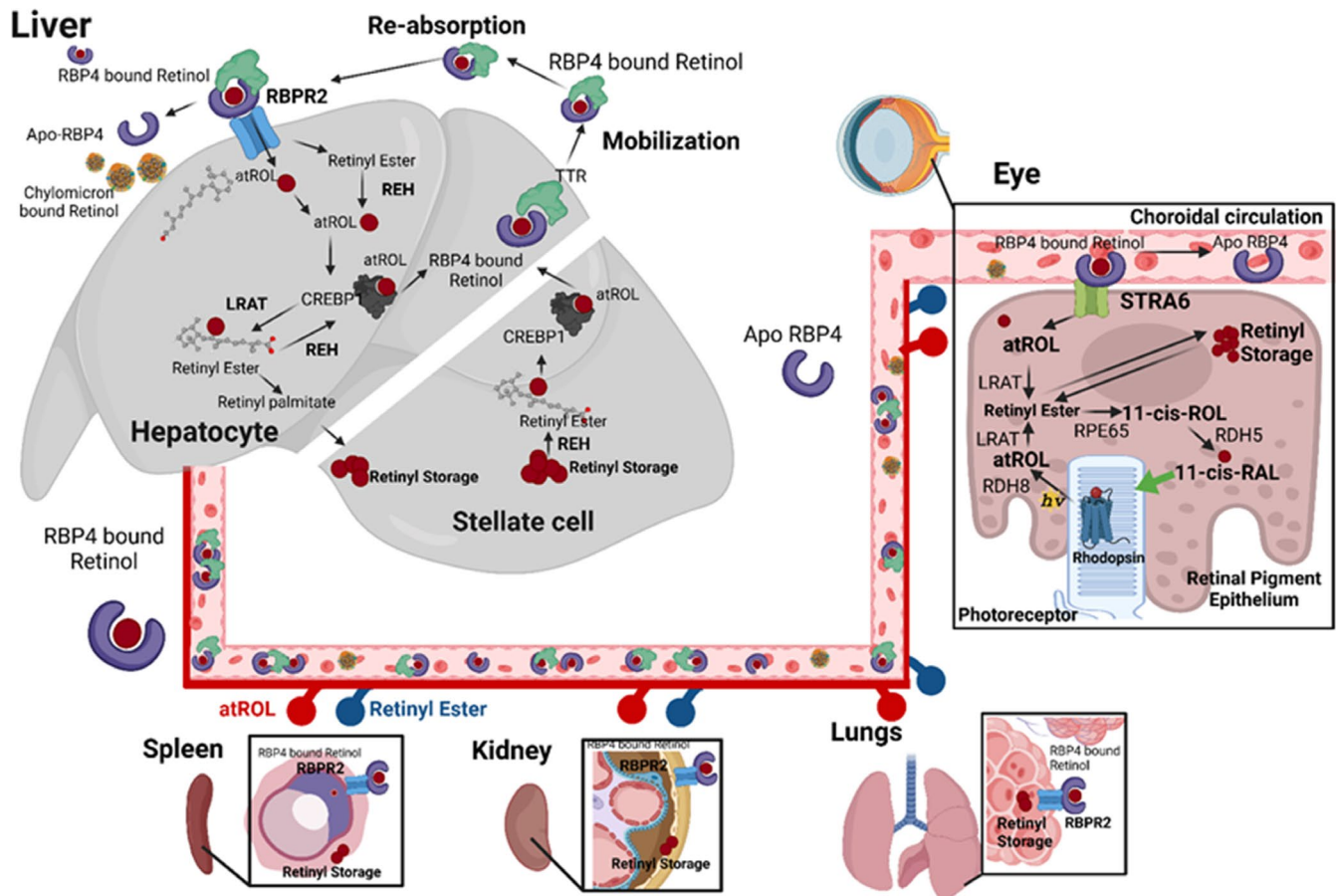
FIGURE 9 Schematic representation outlining the proposed role of the vitamin A receptor RBPR2 in maintaining whole-body retinoid homeostasis. The vitamin A receptor RBPR2 that is expressed in the liver and multiple non-ocular tissues is proposed to be involved in the re-absorption of circulatory ROL from RBP4 protein. This function of RBPR2 is important in maintaining a sufficient retinoid/retinyl ester pool in peripheral tissues for whole-body retinoid homeostasis. This mechanism is also critical for the re-distribution of stored ROL/RE to the eye during periods of fasting or during insufficient dietary vitamin A intake, in the continuous support of chromophore production and phototransduction.

of apoprotein opsin, which constitutively stimulates the phototransduction cascade though stimulation of transducin signaling, where disruption of transducin signaling partially rescues the retinal degenerative phenotype.[15] In a study investigating the phenotypic effects of $Stra6^{-/-}$ mice, which disrupts not only the intake of ROL from circulatory RBP4-ROL into the RPE but also the subsequent generation of the 11-*cis*-retinal chromophore, these mice exhibited elevated concentrations of apoprotein opsin and retinal degeneration much like $Rpe65^{-/-}$ mice, but additionally mislocalization of rod and cone opsins within the photoreceptors.[33] These observations in $Stra6^{-/-}$ and $Rpe65^{-/-}$ mice were also reflected in $Rbpr2^{-/-}$ mice, where significant rhodopsin mislocalization was observed in these mice fed VAS or VAD diets but not in WT mice even on the VAD diet (Figure 8A,G). Moreover, studies examining the phenotypic effects of $Stra6^{-/-}$ mice additionally studied the effects of applying pharmacological doses of vitamin A as a means of rescuing the ocular phenotypes

in these mice. These studies show that interventions with high doses of ROL increase the total retinoid content found within ocular tissues, despite lacking a vitamin A membrane receptor to access circulatory RBP4-ROL due to its lack of functional STRA6. This is a result that was also reflected in $Rbpr2^{-/-}$ mice where a VAS diet is able to supplement systemic retinol/RE levels despite the disruption of vitamin A homeostasis through loss of RBPR2.[29,33] As mentioned above, the retinoid delivery system in mammalian organisms exhibits plasticity in redundancy, where chylomicron transport of RE originating from the diet can act as a possible alternate pathway for delivering retinoids to systemic tissues (Figure 9).[19]

Our study has certain limitations, which could be addressed in the future by generating novel mouse models and subjecting them to variable dietary vitamin A supplementation. Our observation of higher apo-RBP4 protein in the serum of $Rbpr2^{-/-}$ mice was an unexpected observation, which could be indicative of either enhanced

Rbp4 transcription or reduced serum apo-RBP4 clearance. Although published studies indicate that circulatory RBP4 is predominantly expressed in and secreted from the liver in the physiological state, RBP4 is also expressed in significant quantities in adipose tissue in mammals.[20] Through generation of novel liver and adipose-specific *Rbpr2* knockout mice, we would be able to investigate the yet unanswered questions implicated by this study. For example, the mechanism(s) behind the regulation of RBP4–ROL complex in physiological conditions, the tissue-specific origins (liver, adipose, or otherwise) of higher serum apo-RBP4 protein in pathological conditions,[20,43,44] and the tissue re-distribution of unabsorbed ROL. We believe that these unanswered questions necessitate the need for tissue-specific knockout mouse models for RBPR2 and the need for further investigations of the pathologies observed in this study. Therefore, we are currently generating liver- and adipose-conditional *Rbpr2*$^{-/-}$ mice. Second, ocular VA-deficiency (VAD) is a known cause of reversible night blindness in humans, and is attributed to decreased chromophore concentrations affecting rod and cone photoreceptor cell function.[33,45,46,47,48] However, solely, chromophore-deficient mouse mutants do not necessarily exhibit the photoreceptor OS degenerative phenotype of VAD eyes.[46,47] Conversely, prolonged nutritional VAD is associated with irreversible photoreceptor cell degeneration, the mechanisms of which remain unknown.[49,50] Seminal work by Dowling and Wald showed that long-term VAD in rats affect rhodopsin concentrations and eventually results in a 50% reduction in size of photoreceptor outer segment length.[51–53] These ocular defects, which eventually progress to photoreceptor OS degeneration, can be rescued by the injection of all-*trans*-retinol.[51] Surprisingly, how the eyes adapt to changes in dietary vitamin A status and the molecular events associated with photoreceptor OS degeneration in severe dietary VA-deficiency conditions are still unknown. Thus, the *Rbpr2*$^{-/-}$ mouse model could likely serve in the future to answer these outstanding questions.

Given that RBPR2 is hypothesized to function as a regulator of whole-body vitamin A homeostasis and that *Rbpr2*$^{-/-}$ mice display similar ocular phenotypes as other mouse models with disrupted chromophore generation, our study indicates that the vitamin A receptor, RBPR2, is an important facilitator of whole-body retinoid homeostasis in the support of visual function, under variable conditions of dietary vitamin A intake.

AUTHOR CONTRIBUTIONS

Conceptualization, G.P.L.; writing-original draft preparation, G.P.L., R.R., and M.L., performed experiments, R.R., A.L., S.M., and M.L., manuscript writing, review, and editing, G.P.L., R.R., S.M., and M.L.; supervision, G.P.L.; project administration, G.P.L.; funding acquisition, G.P.L. All authors have read and agreed to the published version of the manuscript.

DISCLOSURES

The authors declare no conflict of interest. The funders had no role in the design of the study; in the collection, analyses, or interpretation of data; in the writing of the manuscript, or in the decision to publish the results.

DATA AVAILABILITY STATEMENT

Data sharing is not applicable to this article as no datasets were generated or analyzed in this study. Mice lines and reagents are available from the corresponding author upon reasonable request.

ORCID

Rakesh Radhakrishnan https://orcid.org/0000-0003-3865-0220
Matthias Leung https://orcid.org/0000-0002-8378-8272
Anjelynt Lor https://orcid.org/0009-0004-9658-756X
Swati More https://orcid.org/0000-0002-8733-2029
Glenn P. Lobo https://orcid.org/0000-0003-2698-1989

REFERENCES

1. Carazo A, Macáková K, Matoušová K, Krčmová LK, Protti M, Mladěnka P. Vitamin A update: forms, sources, kinetics, detection, function, deficiency, therapeutic use and toxicity. *Nutrients*. 2021;13(5):1703.
2. Ask N M, Leung M, Radhakrishnan R, Lobo GP. Vitamin A transporters in visual function: a mini review on membrane receptors for dietary vitamin A uptake, storage, and transport to the eye. *Nutrients*. 2021;13(11):3987.
3. Lobo GP, Amengual J, Palczewski G, Babino D, von Lintig J. Mammalian carotenoid-oxygenases: key players for carotenoid function and homeostasis. *Biochim Biophys Acta*. 2012;1821(1):78-87.
4. Kiser PD, Palczewski K. Pathways and disease-causing alterations in visual chromophore production for vertebrate vision. *J Biol Chem*. 2021;296:100072.

5. Palczewski K, Kiser PD. Shedding new light on the generation of the visual chromophore. *Proc Natl Acad Sci USA*. 2020;117(33):19629-19638.

6. Reboul E, Borel P. Proteins involved in uptake, intracellular transport and basolateral secretion of fat-soluble vitamins and carotenoids by mammalian enterocytes. *Prog Lipid Res*. 2011;50(4):388-402.

7. Harrison EH. Carotenoids, β-Apocarotenoids, and Retinoids: the long and the short of it. *Nutrients*. 2022;14(7):1411.

8. Harrison EH. Mechanisms of transport and delivery of vitamin A and carotenoids to the retinal pigment epithelium. *Mol Nutr Food Res*. 2019;63(15):e1801046.

9. Harrison EH. Mechanisms involved in the intestinal absorption of dietary vitamin A and provitamin A carotenoids. *Biochim Biophys Acta*. 2012;1821(1):70-77.

10. Lobo GP, Hessel S, Eichinger A, et al. ISX is a retinoic acid-sensitive gatekeeper that controls intestinal beta,beta-carotene absorption and vitamin A production. *FASEB J*. 2010;24:1656-1666.

11. Lobo GP, Amengual J, Baus D, Shivdasani RA, Taylor D, von Lintig J. Genetics and diet regulate vitamin A production via the homeobox transcription factor ISX. *J Biol Chem*. 2013;288:9017-9027.

12. Widjaja-Adhi M, Lobo GP, Golczak M, von Lintig J. A diet responsive regulatory network controls intestinal fat-soluble vitamin and carotenoid absorption. *Hum Mol Genet*. 2015;24:3206-3219.

13. Tian H, Sakmar TP, Huber T. The energetics of chromophore binding in the visual photoreceptor rhodopsin. *Biophys J*. 2017;113:60-72.

14. Fan J, Rohrer B, Frederick JM, Baehr W, Crouch RK. Rpe65$^{-/-}$ and Lrat$^{-/-}$ mice: comparable models of leber congenital amaurosis. *Invest Ophthalmol Vis Sci*. 2008;49:2384-2389.

15. Woodruff ML, Wang Z, Chung HY, Redmond TM, Fain GL, Lem J. Spontaneous activity of opsin apoprotein is a cause of Leber congenital amaurosis. *Nat Genet*. 2003;35(2):158-164.

16. Jones GJ, Cornwall MC, Fain GL. Equivalence of background and bleaching desensitization in isolated rod photoreceptors of the larval tiger salamander. *J Gen Physiol*. 1996;108(4):333-340.

17. Fan J, Woodruff ML, Cilluffo MC, Crouch RK, Fain GL. Opsin activation of transduction in the rods of dark-reared Rpe65 knockout mice. *J Physiol*. 2005;568(Pt 1):83-95.

18. Quadro L, Blaner WS, Salchow DJ, et al. Impaired retinal function and vitamin A availability in mice lacking retinol-binding protein. *EMBO J*. 1999;18(17):4633-4644.

19. Steinhoff JS, Lass A, Schupp M. Retinoid homeostasis and beyond: how retinol binding protein 4 contributes to health and disease. *Nutrients*. 2022;14(6):1236.

20. Kawaguchi R, Yu J, Honda J, et al. A membrane receptor for retinol binding protein mediates cellular uptake of vitamin a. *Science*. 2007;315(5813):820-825.

21. Kawaguchi R, Yu J, Wiita P, Honda J, Sun H. An essential ligand-binding domain in the membrane receptor for retinol-binding protein revealed by large-scale mutagenesis and a human polymorphism. *J Biol Chem*. 2008;283(22):15160-15168.

22. Kawaguchi R, Yu J, Wiita P, Ter-Stepanian M, Sun H. Mapping the membrane topology and extracellular ligand binding domains of the retinol binding protein receptor. *Biochemistry*. 2008;47(19):5387-5395.

23. Radhakrishnan R, Leung M, Roehrich H, et al. Mice lacking the systemic vitamin A receptor RBPR2 show decreased ocular Retinoids and loss of visual function. *Nutrients*. 2022;14(12):2371.

24. Radhakrishnan R, Leung M, Solanki AK, Lobo GP. Mapping of the extracellular RBP4 ligand binding domain on the RBPR2 receptor for vitamin A transport. *Front Cell Dev Biol*. 2023;11:1105657. doi:10.3389/fcell.2023.1105657

25. Shi Y, Obert E, Rahman B, Rohrer B, Lobo GP. The retinol binding protein receptor 2 (Rbpr2) is required for photoreceptor outer segment morphogenesis and visual function in zebrafish. *Sci Rep*. 2017;7(1):16207.

26. Lobo GP, Pauer G, Lipschutz JH, Hagstrom SA. The retinol-binding protein receptor 2 (Rbpr2) is required for photoreceptor survival and visual function in the zebrafish. *Adv Exp Med Biol*. 2018;1074:569-576.

27. Solanki AK, Kondkar AA, Fogerty J, et al. A functional binding domain in the Rbpr2 receptor is required for vitamin A transport, ocular retinoid homeostasis, and photoreceptor cell survival in zebrafish. *Cells*. 2020;9(5):1099.

28. Amengual J, Zhang N, Kemerer M, Maeda T, Palczewski K, von Lintig J. STRA6 is critical for cellular vitamin A uptake and homeostasis. *Hum Mol Genet*. 2014;23:5402-5417.

29. Alapatt P, Guo F, Komanetsky SM, et al. Liver retinol transporter and receptor for serum retinol-binding protein (RBP4). *J Biol Chem*. 2013;288(2):1250-1265.

30. Mattapallil MJ, Wawrousek EF, Chan CC, et al. The Rd8 mutation of the Crb1 gene is present in vendor lines of C57BL/6N mice and embryonic stem cells, and confounds ocular induced mutant phenotypes. *Invest Ophthalmol Vis Sci*. 2012;53:2921-2927.

31. Ramkumar S, Parmar VM, Samuels I, Berger NA, Jastrzebska B, von Lintig J. The vitamin A transporter STRA6 adjusts the stoichiometry of chromophore and opsins in visual pigment synthesis and recycling. *Hum Mol Genet*. 2022;31:548-560.

32. Ross AC. Diet in vitamin A research. *Methods Mol Biol*. 2010;652:295-313.

33. Cornwall MC, Jones GJ, Kefalov VJ, Fain GL, Matthews HR. Electrophysiological methods for measurement of activation of phototransduction by bleached visual pigment in salamander photoreceptors. *Methods Enzymol*. 2000;316:224-252.

34. Yang Q, Graham TE, Mody N, et al. Serum retinol binding protein 4 contributes to insulin resistance in obesity and type 2 diabetes. *Nature*. 2005;436(7049):356-362.

35. Kane MA, Napoli JL. Quantification of endogenous retinoids. *Methods Mol Biol*. 2010;652:1-54.

36. Leung M, Radhakrishnan R, Lor A, et al. Quantitative analysis of dietary vitamin A metabolites in murine ocular and non-ocular tissues using high-performance liquid chromatography. *J Vis Exp*. 2024;(214).

37. Lobo GP, Biswal MR, Kondkar AA. Editorial: molecular mechanisms of retinal cell degeneration and regeneration. *Front Cell Dev Biol*. 2021;9:667028.

38. Leung M, Steinman J, Li D, et al. The logistical backbone of photoreceptor cell function: complementary mechanisms of dietary vitamin A receptors and rhodopsin transporters. *Int J Mol Sci*. 2024;25(8):4278.

39. Moon J, Ramkumar S, von Lintig J. Genetic dissection in mice reveals a dynamic crosstalk between the delivery pathways of vitamin A. *J Lipid Res*. 2022;63(6):100215.

40. Patil S, Zamwar UM, Mudey A. Etiology, epidemiology, pathophysiology, signs and symptoms, evaluation, and treatment of vitamin A (retinol) deficiency. *Cureus*. 2023;15(11):e49011.

41. Radhakrishnan R, Lor A, Li D, Mudaliar D, Lobo GP. Methodology for studying interactions of vitamin A membrane receptors and opsin protein with their ligands in generating the Retinylidene protein. *J Vis Exp*. 2024;(212).

42. Moon J, Zhou G, Jankowsky E, von Lintig J. Vitamin A deficiency compromises the barrier function of the retinal pigment epithelium. *PNAS Nexus*. 2023;2(6):pgad167. doi:10.1093/pnasnexus/pgad167

43. Huang D, Qian X, Chen J, Peng Y, Zhu Y. Factors and molecular mechanisms of vitamin A and childhood obesity relationship: a review. *J Nutr Sci Vitaminol (Tokyo)*. 2023;69(3):157-163.

44. Samardzija M, von Lintig J, Tanimoto N, et al. R91w mutation in Rpe65 leads to milder early-onset retinal dystrophy due to the generation of low levels of 11-cis-retinal. *Hum Mol Genet*. 2008;17:281-292.

45. Song P, Adeloye D, Li S, et al. The prevalence of vitamin A deficiency and its public health significance in children in low- and middle-income countries: a systematic review and modelling analysis. *J Glob Health*. 2023;13:04084.

46. Hu Y, Chen Y, Moiseyev G, Takahashi Y, Mott R, Ma JX. Comparison of ocular pathologies in vitamin A-deficient mice and RPE65 gene knockout mice. *Invest Ophthalmol Vis Sci*. 2011;52:5507-5514.

47. Dewett D, Lam-Kamath K, Poupault C, Khurana H, Rister J. Mechanisms of vitamin A metabolism and deficiency in the mammalian and fly visual system. *Dev Biol*. 2021;476:68-78.

48. Pereira A, Adekunle RD, Zaman M, Wan MJ. Association between vitamin deficiencies and ophthalmological conditions. *Clin Ophthalmol*. 2023;17:2045-2062.

49. Dewett D, Labaf M, Lam-Kamath K, Zarringhalam K, Rister J. Vitamin A deficiency affects gene expression in the Drosophila melanogaster head. *G3 (Bethesda)*. 2011;11(11):jkab297.

50. Katz ML, Chen DM, Stientjes HJ, Stark WS. Photoreceptor recovery in retinoid-deprived rats after vitamin A replenishment. *Exp Eye Res*. 1993;56:671-682.

51. Dowling JE, Wald G. Vitamin A deficiency and night blindness. *Proc Natl Acad Sci USA*. 1958;44:648-661.

52. Dowling JE, Wald G. The biological function of vitamin A acid. *Proc Natl Acad Sci USA*. 1960;46:587-608.

53. Landers GM, Olson JA. Rapid, simultaneous determination of isomers of retinal, retinal oxime and retinol by high-performance liquid chromatography. *J Chromatogr*. 1988;438(2):383-392.

SUPPORTING INFORMATION

Additional supporting information can be found online in the Supporting Information section at the end of this article.